AIAA 2003-4161

DYNAMIC SEPARATION CONTROL IN A LOW-SPEED ASYMMETRIC DIFFUSER WITH VARYING DOWNSTREAM BOUNDARY CONDITION

Samantha H. Feakins, Douglas G. MacMartin, and Richard M. Murray
California Institute of Technology
Pasadena, California

Abstract

This paper presents an experimental investigation into the effect of a varying downstream boundary condition on dynamic separation control in a two-dimensional low-speed asymmetric diffuser. The potential for coupling between the downstream boundary condition and the separation dynamics is relevant, for example, in using separation control to enable more aggressive serpentine aircraft inlets, where the compressor may be close to the separation point. Separation control in the experiment is obtained using spanwise unsteady forcing from a single tangential actuator located directly upstream of the separation point. The downstream boundary condition simulates the dominant quasi-steady and reflection characteristics of a compressor. Although the boundary condition affects the uncontrolled pressure recovery, the optimal forcing frequency is shown to depend only on the mass flow rate and not on either the presence, impedance, or location of the downstream boundary condition. At the conditions tested herein, we therefore conclude that the mechanism underlying dynamic separation control is *local* in nature, and is not influenced by global system dynamics.

1 Introduction

The desire to minimize flow separation and its detrimental effect on performance has long been a design issue with flow devices. Both passive and active methods of separation control have been proposed, including vortex generators, boundary layer suction, and tangential blowing. Zero-mean unsteady forcing at the separation point has been demonstrated to control separation using significantly less actuation authority than steady blowing or suction.[1,2]

Unsteady separation control has been demonstrated in a wide range of flow geometries and conditions. Unsteady forcing achieves an improvement in separation behavior by modulating the vorticity that continually accumulates at the separation point.[3] However, a complete explanation and analytical model that predicts the optimal forcing frequency and resulting pressure recovery has not yet been developed, and the parametric dependence of these variables has therefore been assumed based on empirical results. The optimal forcing frequency depends on the local flow velocity and the characteristic length of the separated flow, but is typically assumed not to depend on any global system dynamics. Previous experiments in a two-dimensional diffuser indicate that overall system dynamics may impact the dynamics of the separation region. For example, it has been shown that the acoustics of a duct to which a diffuser is connected has a significant effect on the unsteady flow within the diffuser.[4] The potential for such coupling between separation and global diffuser dynamics is of particular importance when an aggressive (short) diffuser is closely coupled to a downstream boundary condition, as occurs in serpentine aircraft inlets. This type of aggressive diffuser, which may enable significant reductions in aircraft size, necessitates effective separation control to stabilize the flow before the compressor face. A preliminary assessment of actuator authority requirements indicates that unsteady control of separation dynamics for aggressive inlet geometry may be viable.[5]

To investigate the coupling of system and separation dynamics in a two-dimensional asymmetric diffuser, a downstream boundary condition simulating the dominant quasi-steady and reflection characteristics of a compressor was constructed. The boundary condition (compressor or simulated) has both a quasi-static and a possible dynamic effect on the separated region. The quasi-static effect reduces the severity of the separation and improves pressure recovery. To assess whether the boundary condition affects the pressure recovery *dynamics* during active separation control, the influence of excitation frequency on pressure recovery (C_p) was evaluated as a function of boundary condition location and impedance.

The following sections present the relevant theory and experimental setup, followed by the experimental results. The effect of the location and impedance of the boundary condition on the performance of dynamic separation control is evaluated by moving the boundary condition between three pre-set locations and changing the solidity of the steel plating used to simulate the compressor. Although there is a quasi-steady effect on pressure recovery, the optimal forcing frequency is shown to be independent of boundary condition location and impedance.

2 Boundary Condition Simulation

The mechanisms underlying unsteady separation control are not fully understood. Although there have been extensive empirical and some numerical validations, there are limited analytical results. Scaling is assumed to depend only on the non-dimensional momentum coefficient and non-dimensional forcing frequency. A simplified model of separation control is based on the modulation of the vorticity that continually accumulates at the separation point; periodic forcing causes vortex shedding at a higher frequency and hence lower circulation than would otherwise occur. The pressure recovery in turn depends on the size of the vortices at the diffuser exit. This description has been validated by a direct numerical simulation with a dissipative downstream boundary condition. However, a reflective downstream boundary can influence the shedding of vorticity, and therefore may be relevant in applications where a downstream boundary condition is closely coupled to the separation point.

The experiments are based on the assumption that the dominant effects of the compressor can be adequately modeled by a downstream boundary condition composed of perforated steel plate and honeycomb. There are two characteristics of the downstream boundary condition that influence the separation region; a quasi-steady flow redistribution that reduces the severity of the separation, and its dynamic acoustic reflection coefficient that influences the global system modes of the diffuser. The compressor creates axial exit flow and a pressure rise related to mass flow via the compressor characteristic:

$$\frac{P_2 - P_1}{\rho U^2} = \psi\left(\frac{U}{u}\right) = \psi(\phi) \tag{1}$$

The downstream boundary condition used in the experiment creates axial exit flow through the honeycomb and a pressure drop dependent on the impedance of the screen, K, and the mass flow:

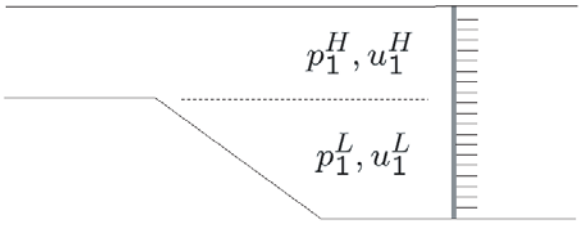

Figure 1: Schematic of boundary condition influence for fully separated flow.

$$\Delta P = -K\left(\frac{1}{2}\rho U^2\right) \tag{2}$$

For both the relevant quasi-steady and dynamic characteristics of the boundary condition, it is the slope of the relationship between ΔP and u that matters, not the absolute pressure rise or drop. Hence, choose

$$K = -\frac{1}{\phi}\frac{d\psi}{d\phi} \tag{3}$$

To compare the quasi-steady flow redistribution, consider the extreme case where the incoming flow does not diffuse at all, and the flow has velocity u_1^H over part of the boundary condition face and u_1^L over the remainder, imparted by the separation; this is shown schematically in Figure 1. Then the boundary condition creates a pressure gradient between these regions given by :

$$\begin{aligned} P_1^L - P_1^H &= \rho\overline{u}\left(\frac{1}{\phi}\frac{\mathrm{d}\psi}{\mathrm{d}\phi}\right)(u^H - u^L) \\ &= -\rho\overline{u}K(u^H - u^L) \end{aligned} \tag{4}$$

The acoustic reflection coefficient for the compressor or downstream boundary condition is:

$$\frac{P_R}{P_I} = \frac{\alpha}{1+\alpha} \tag{5}$$

where

$$\begin{aligned} \alpha &= \frac{1}{2}K\frac{u}{c} \\ &= \frac{1}{2}\left(\frac{1}{\phi}\frac{\mathrm{d}\psi}{\mathrm{d}\phi}\right)\frac{u}{c} \end{aligned} \tag{6}$$

This expression ignores the area change across the compressor, which leads to additional terms in the equation.[6] For a more complete analysis see Sajben *et al.*;[7] the reflection coefficient for realistic compressors is roughly 0.2.

Using a cubic expression for the compressor characteristic[8] leads to a linear increase in $K_c = -(1/\phi)(\frac{d\psi}{d\phi})$ starting with zero at the peak compression (near stall) and increasing to $K_c < 2$ over a realistic operating range. For a compressor face Mach number of 0.5, the reflection coefficient of 0.2 corresponds to $K_c = 1$ or $K_c M = 0.5$.

The impedance of a perforated plate of solidity s is approximately[9]

$$K = \frac{(s + \sqrt{s/2})^2}{1 - s} \tag{7}$$

Thus for the solidity used herein (see the next section) ranging from $0.37 \leq s \leq 0.67$, $1 \leq K \leq 5$. Conditions close to those of a typical compressor at a Mach number of 0.5 can therefore be achieved with a high solidity perforated plate and the lower flow speeds used herein.

The boundary condition creates two types of modes that could interact with the unsteady separation dynamics. The frequency of the acoustic modes in the duct is a function of the length from the inlet to the boundary condition, and therefore varies with the position of the boundary condition, but not with mass flow (although the strength of the reflection, and therefore the importance of the resonance, may vary with mass flow). A second possible dynamic interaction with the downstream boundary condition may result from acoustic feedback much like the Rossiter mechanism in cavity flow instabilities. Vorticity is periodically shed at the separation point and convected downstream, which can result in a reflected acoustic wave that forces the shedding. The time scale of this process is dominated by the convection time rather than the acoustic propagation, and therefore scales with both the location of the boundary condition with respect to the separation point, and the mean flow velocity.

Our objective is to understand whether these system dynamics influence the control of separation, or whether the mechanisms underlying unsteady separation control are purely local. The boundary condition clearly affects the separation in a quasi-steady manner, and we therefore need to distinguish between the quasi-steady and dynamic influence of the boundary condition. The former we expect to change the unforced pressure recovery, and therefore to change the pressure recovery for any forcing frequency. However, changes in the optimum forcing frequency indicate a change in the dynamics being controlled. The approach, therefore, is to understand how the optimal forcing frequency varies with mass flow rate, boundary condition location, and boundary condition impedance; the local dynamics are influenced only by the first of these, while the global system dynamics are a function of all three. Independently varying boundary condition and mass flow further allows distinguishing between different dynamic effects.

3 Experiment

The experiments were performed in an asymmetric diffuser shown in Figure 2, with air flow at Reynolds numbers approximately $3.5 * 10^4 < \mathrm{Re} < 7.4 * 10^4$ where Reynolds number $\mathrm{Re} = \frac{xU\rho}{\mu}$ is based on inlet width $x = 0.064$ m, inlet velocity U m/s, ideal density $\rho = 1.2$ kg/m^3 and ideal dynamic viscosity of the fluid μ=1.80e-5 Ns/m^2. The experimental apparatus has dimensions 6.4 cm wide by 17.8 cm high by 58 cm long upstream of the asymmetric diffuser and 17.8 cm wide by 17.8 cm wide by 27.7 cm long downstream of the diffuser. Between the upstream and downstream sections, separation is achieved by an expansion on one side of the duct angled out at 23 degrees. As shown in Figure 3, the downstream portion of the rig is composed of three interchangeable 7.7 cm long duct sections with the 4.6 cm long boundary condition, composed of honeycomb and perforated steel plate, as an additional fourth section. For the baseline case, unconstrained flow with no boundary condition, a 4.6 cm long duct section is put in place of the boundary condition. The downstream portion of the rig precedes a 35 cm long fiberglass duct which transitions from the 17.8 cm square duct to a 17.3 cm diameter circle attached to an Able Corporation 29680 axial flow turbine. A speaker-driven slot at the separation point provided the unsteady forcing for separation control. The slot is one quarter-inch wide, spanning the entire width of the diffuser, and angled to provide nearly tangential injection during the blowing phase of the excitation. The separation point is at the upstream lip of the slot. An 8-inch speaker mounted in a cavity behind the slot provides excitation; sinusoidal excitation was considered ranging from 30 to 400 Hz.

Static pressure taps mounted on the four side walls, both upstream and downstream of the diffuser, were averaged and connected to two Honeywell 163PC01D36 differential pressure transducers to measure the mean as well as unsteady pressure recovery. The sampling rate was 1 kHz. After a settling time of 2 seconds, 3 seconds of data were collected and averaged for each data point. Data was taken for data points S $\otimes$ L where S = boundary solidities = [37%, 55%,67%] and L = boundary locations = [0", 3.5",6.5"] from end of expansion ramp.

Smoke generated by a V-920 Visual Effects fog machine was used to visualize flow patterns at the

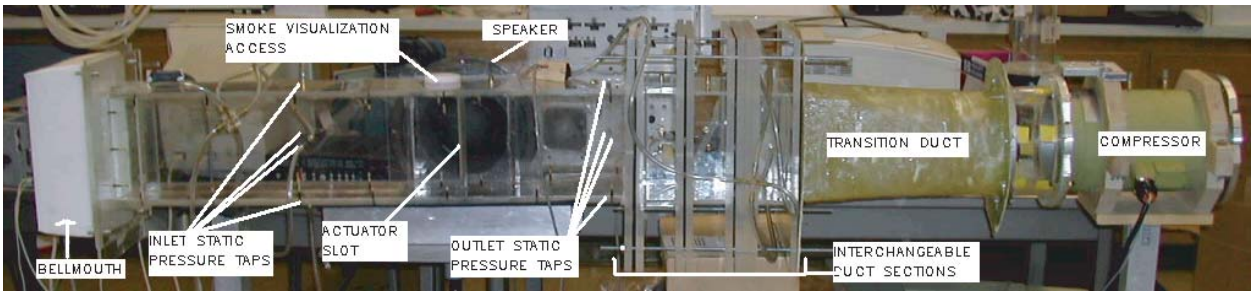

Figure 2: Diffuser.

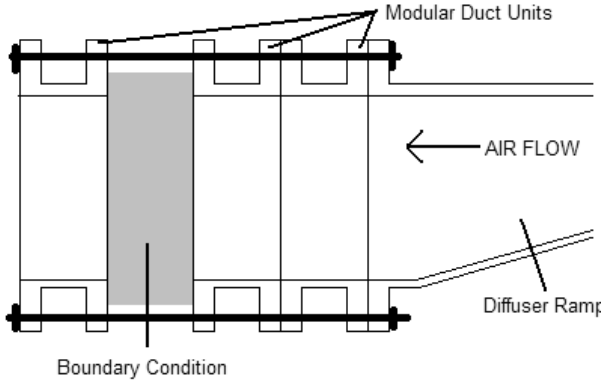

Figure 3: Schematic of Modular Units in Diffuser.

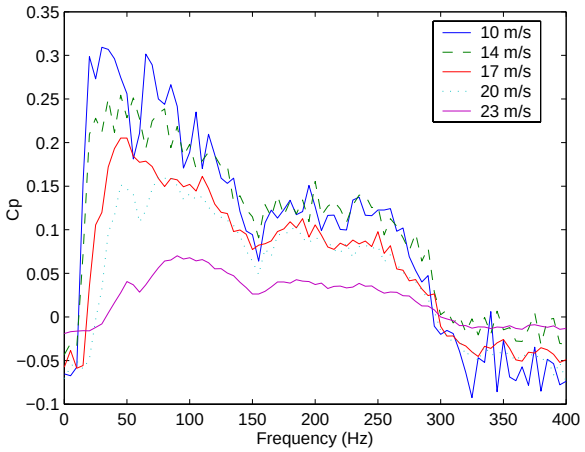

Figure 4: Effect of Actuation on C_p with No Downstream Boundary Condition.

separation point while varying the level of actuation and the location and impedance of the boundary condition. A high speed camera, laser sheet, and Phantom data acquisition program were utilized in conjunction with the smoke visualization.

4 Experimental Results

4.1 Optimal Forcing Frequency and Amplitude

We begin with the baseline case, shown in Figure 4, evaluating separation control via non-dimensional pressure recovery with no downstream boundary condition. As expected, the optimal forcing frequency increases as mass flow through the compressor is increased. For constant speaker voltage, the effectiveness of actuation decreases with increased mass flow. The actuator calibration is not included in these plots; constant speaker voltage does not imply constant C_μ. The variation is within roughly $\pm 15\%$ between 30 and 200 Hz and thus the optimum frequency for constant voltage is close to the optimum for constant C_μ.

Similar dependence of the optimal forcing frequency on mass flow was observed for all boundary condition locations and impedances.

As shown in Figure 5, increased speaker power typically reduces losses until a saturation limit is reached but does not change the optimal forcing frequency when the amplification is within its effective range. At low speaker voltage, pressure recovery becomes less consistent.

4.2 Impedance

Mass flow ϕ through the boundary condition was held constant for varying boundary solidity. Assuming that the loss through the bellmouth inlet scales with dynamic pressure:

$$\Delta P = \alpha \left(\frac{1}{2} \rho u^2 \right) \tag{8}$$

then constant inlet pressure corresponds to constant mass flow. The effect of impedance on pressure recovery holding ϕ constant is seen in Figure 6.

Note that the impedance of the boundary condition has no significant effect on either the magnitude or trend of the pressure recovery when mass flow through the boundary condition is held constant.

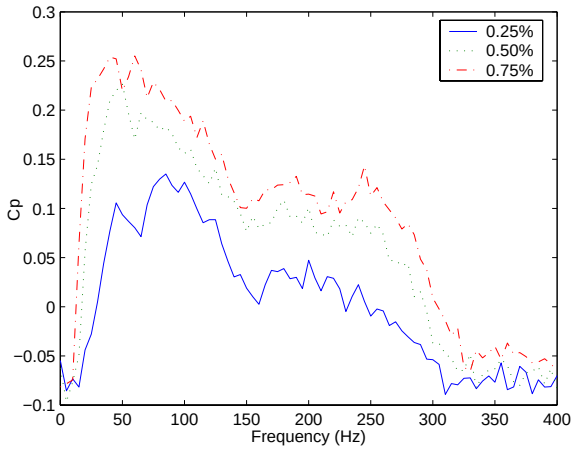

Figure 5: Effect of Amplitude on C_p: 37% Solidity Downstream Boundary Condition 6.5" from End of Diffuser.

Additional plots showing similar results for other boundary condition locations with varying impedance are shown in Figure 10 and Figure 11.

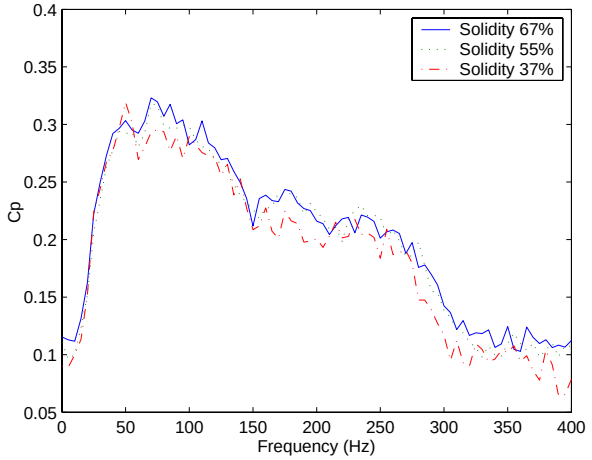

Figure 6: Effect of Impedance on C_p: 0" from End of Diffuser.

4.3 Location

The location of the downstream boundary condition was set at increments of 0", 3.5", and 6.5" away from the end of the asymmetric expansion that initially induced flow separation and vortex formation. As shown in Figure 7, location impacted nominal pressure recovery quasi-steadily but had no impact on the unsteady control of separation dynamics. Also, the optimal forcing frequency remained unchanged.

Additional plots showing similar results for other

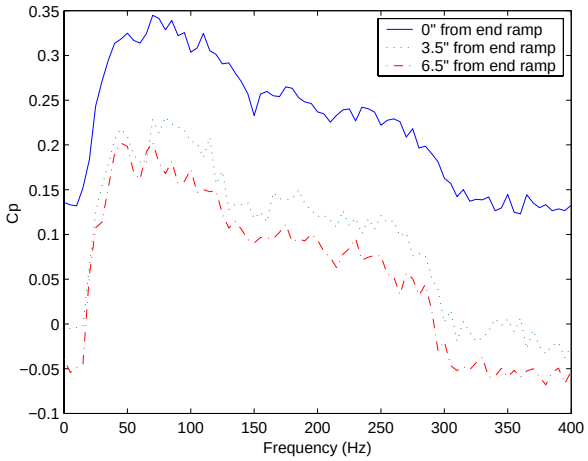

Figure 7: Effect of Location on C_p: 67% Solidity Downstream Boundary Condition.

impedances with varying boundary condition location are shown in Figure 12 and Figure 13.

5 Error

Sources of error included short-term fluctuations in the sinusoidal mean and long-term fluctuations in the static pressure readings. The former was minimized by a settling period of two seconds and an averaging period of three seconds for each data point, taken at 1 kHz. RMS error for these sources was calculated and found to be within a reasonable range for the comparisons presented in this paper, consistent with the scatter between neighboring frequency points observed in the plots.

Properties of the speaker contributed to error. At frequencies less than approximately 30Hz, the speaker response is nonlinear and does not produce sinusoidal output but rather a mixture of low frequencies. Although data in this frequency range is provided in the plots, it should be considered an approximation of the transition from no actuation.

Error was incurred while holding mass flow constant for varying screen impedance via holding inlet pressure constant. Pressure transducer fluctuations while matching inlet pressures contributed to this error. In addition, although the mass flow rate was adjusted for given boundary condition location and impedance, the sweep of excitation frequency was done with constant compressor speed, not mass flow. As separation losses are reduced, the mass flow rate will increase slightly.

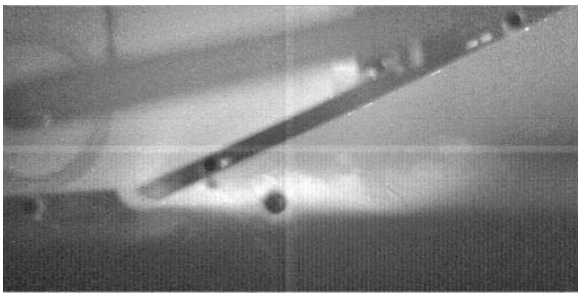

Figure 8: Top View of Diffuser with No Downstream Boundary Condition and No Forcing.

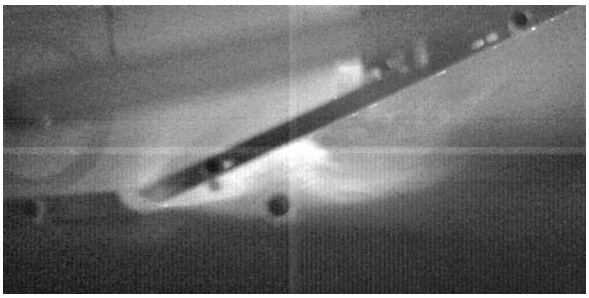

Figure 9: Top View of Diffuser with No Downstream Boundary Condition at Optimal Forcing.

6 Flow Visualization

Smoke was used in conjunction with high-speed photography and a laser sheet to visualize flow patterns at the separation point while varying the location and impedance of the boundary condition. The photography was done with a Phantom 5 camera at 2000 frames per second, with a resolution of 1024x512 pixels. Smoke was air-driven from a holding chamber into the duct at the separation point in order to achieve a controlled smoke stream.

The effect of actuation, at optimal forcing frequency, on separation control was evident when no downstream boundary condition was in place, with a visible change in the attachment angle of the smoke to the diffuser wall. This effect can be seen in Figure 8 and Figure 9. We also observe that the "size" of a typical shed vortex is clearly visible in Figure 9. An increase in the magnitude of actuation continued to increase attachment until a saturation amplitude was reached.

The unforced and forced cases look similar to each other when a boundary condition is present, with a slight increase in the expansion angle for both cases. The slight increase in expansion angle is expected due to the increase in pressure recovery even in the unforced case when the boundary condition is present.

7 Concluding Remarks

Unsteady forcing at the separation point is effective at improving overall metrics such as diffuser pressure recovery by modulating the vorticity that accumulates at the separation point so that more frequent, smaller vortex structures are shed. The optimal forcing frequency has typically been assumed to depend only on *local* parameters: the flow speed, and the length of the separated region, and not on *global* system modes. The purpose of this experiment was to gain information on whether the mechanism underlying dynamic separation control is influenced by global system dynamics, or purely by local dynamics at the separation point; this understanding is critical when the separation point is close to the downstream boundary condition as might happen in aggressive serpentine inlets. The experiment used a downstream boundary condition composed of honeycomb and perforated steel plate to simulate the quasi-static and dynamic characteristics of a compressor. The boundary condition enabled the evaluation of C_p as a function of forcing frequency for various boundary locations and impedances, and the effect of location and impedance on the optimal forcing frequency.

The optimal forcing frequency of the actuation shifts to a higher value as mass flow through the duct is increased, as expected. However, the optimal forcing frequency does not depend on boundary presence, location, or impedance. Therefore, we conclude that neither the impedance nor the location of the downstream boundary condition influence the mechanism underlying dynamic separation control, although clearly the impedance and location clearly have a quasi-steady influence on the dynamics of separation.

Acknowledgements

Professor Tom Hynes of the University of Cambridge, Department of Engineering suggested the implementation of the compressor. Al Ratner, California Institute of Technology, assisted with flow visualization, and Vikram Mittal, California Institute of Technology collected the flow visualization data. Jeremy Pitts, California Institute of Technology, helped with construction of the experimental apparatus. Sean Humbert, California Institute of Technology, assisted with the data acquisition program. Funding provided by DARPA.

References

[1] Greenblatt, D. and Wygnanski, I. J., "The control of flow separation by periodic excitation,"

Progress in Aerospace Sciences, Vol. 36, 2000, pp. 487–545.

[2] McCormick, D. C., "Boundary Layer Separation Control with Directed Synthetic Jets," *AIAA Aerospace Sciences Conference*, AIAA 2000–0519.

[3] Suzuki, T., Colonius, T., and MacMartin, D. G., "Inverse technique for vortex imaging and its application to feedback flow control," *AIAA Fluid Dynamics Conference*, 2003, AIAA 2003–4260.

[4] Kwong, A. and Dowling, A., "Unsteady Flow in Diffusers," *Journal of Fluids Engineering*, Vol. 116, 1994, pp. 842–847.

[5] MacMartin, D. G., Verma, A., Murray, R. M., and Paduano, J. D., "Active Control of Integrated Inlet/Compression Systems: Initial Results," *ASME Fluids Engineering Division Summer Meeting*, 2001, ASME FEDSM2001-18275.

[6] MacMartin, D. G., "Dynamics and Control of Shock Motion in a Near-Isentropic Inlet," in press *AIAA J. Aircraft*, 2003.

[7] Sajben, M. and Said, H., "Acoustic-Wave/Blade-Row Interactions Establish Boundary Conditions for Unsteady Inlet Flows," *AIAA J. Propulsion and Power*, Vol. 17, No. 5, 2001, pp. 1090–1099.

[8] Moore, F. K. and Greitzer, E. M., "A theory of post-stall transients in axial flow compression systems part I: Development of Equations," *ASME Journal of Engineering for Gas Turbines and Power*, Vol. 108, 1986, pp. 68–76.

[9] Idelchik, I. E., *Handbook of Hydraulic Resistance*, Hemisphere Publishing Corp., New York, 1986.

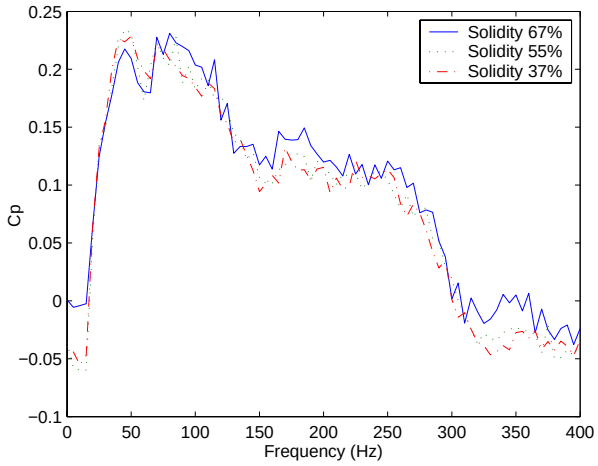

Figure 10: Effect of Impedance on C_p: 3.5" from End of Diffuser.

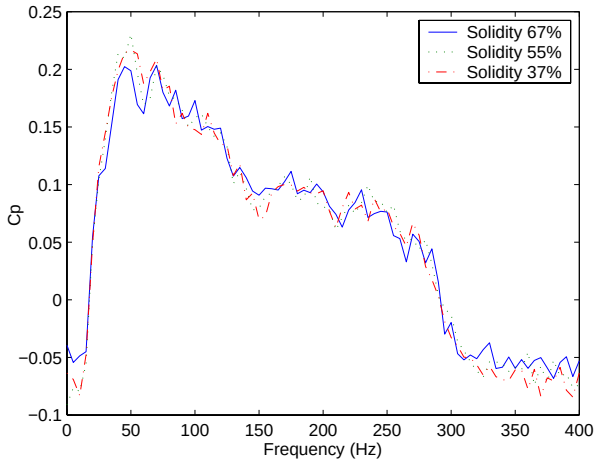

Figure 11: Effect of Impedance on C_p: 6.5" from End of Diffuser.

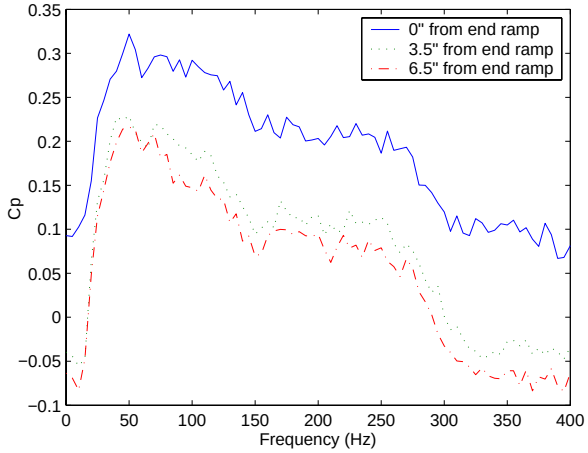

Figure 12: Effect of Location on C_p: 37% Solidity Downstream Boundary Condition.

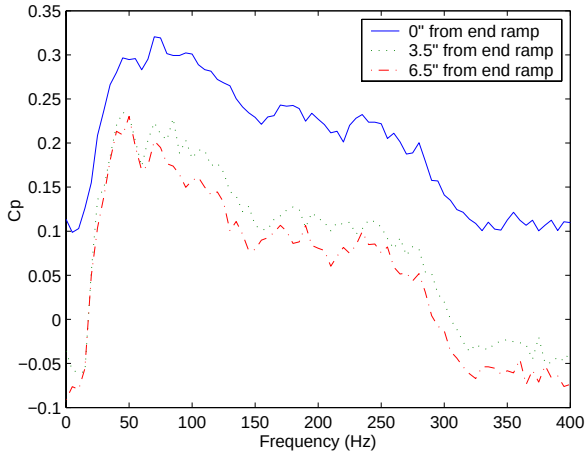

Figure 13: Effect of Location on C_p: 55% Solidity Downstream Boundary Condition.